Biosynthesis of the α-D-Mannosidase Inhibitor (–)-Swainsonine

Shaonan Liu,[1] Zainab Batool,[1] and Yang Hai[1]

[1] *Department of Chemistry and Biochemistry, University of California, Santa Barbara, Santa Barbara, CA, 93106, USA.*

Correspondence and requests for materials should be addressed to Y.H. (*hai@chem.ucsb.edu)*

Abstract (150 words)

(–)-Swainsonine is a polyhydroxylated indolizidine alkaloid with potent inhibitory activity against α-D-mannosidases. In this work, we successfully reconstituted swainsonine biosynthetic pathway both in vivo and in vitro. Our study unveiled an unexpected epimerization mechanism involving two α-ketoglutarate-dependent non-heme iron dioxygenases (SwnH2 and SwnH1), and an unusual imine reductase (SwnN), which displays substrate-dependent stereospecificity. The stereochemical outcome of SwnN-catalyzed iminium reduction is ultimately dictated by SwnH1-catalyzed C8-hydroxylation. We also serendipitously discovered that an *O*-acetyl group can serve as a detachable protecting/directing group, altering the site-selectivity of SwnH2-catalyzed hydroxylation while maintaining the stereoselectivity. Insights gained from the biochemical characterization of these tailoring enzymes enabled biocatalytic synthesis of a new polyhydroxylated indolizidine alkaloid, opening doors to the biosynthesis of diverse natural product-based glycosidase inhibitors.

Introduction

Polyhydroxylated alkaloids, also known as iminosugar alkaloids, are a class of natural products recognized for their potent and selective glycosidase inhibitory activity (**Figure 1a**).[1] These compounds mimic the transition states of glycoside-cleavage reactions, enabling them to bind tightly to glycosidase active sites and effectively inhibit enzymatic function.[2] This distinctive mode of action makes polyhydroxylated alkaloids valuable chemical tools for studying glycosidase-mediated cellular processes and promising candidates for developing therapeutics targeting diseases such as cancer, diabetes, viral infections, and metabolic disorders, where glycosidases play a critical role.[3]

(–)-Swainsonine (SW) is a polyhydroxylated indolizidine alkaloid initially isolated from Darling pea (*Swainsona canescens*)[4] and the fungus *Rhizoctonia leguminicola* (**Figure 1a**).[5] It is also commonly found in spotted locoweeds (e.g. *Astragalus* and *Oxytropis*) and identified as the causative agent of "locoism" in grazing animals.[6] The toxicity of SW arises from its inhibition of lysosomal α-mannosidase, leading to the accumulation of mannose-rich oligosaccharides, a hallmark symptom of the genetic disorder α-mannosidosis.[7] SW is also shown as a potent inhibitor of Golgi α-mannosidase II, an enzyme essential for the maturation of *N*-linked oligosaccharides in newly synthesized glycoproteins.[8,9] As a result, SW was the first glycoprotein processing inhibitor to undergo clinical trials for cancer treatment.[10] Additionally, SW has been explored in the development of therapeutics for viral infections and immunological disorders.[11,12]

Due to its exceptional biological activities and unique structure, SW has garnered significant interest as a synthetic target, spurring the development of diverse synthetic strategies for its total synthesis and that of its analogues.[13-19] However, despite decades of investigations, the mechanical details of SW biosynthesis remains elusive. Harris et al. first demonstrated that SW is derived from L-pipecolic acid (PA) and malonate, and identified an

enigmatic epimerization evet at the ring fusion (C8a position) through feeding studies (**Figure S1**).[20-22] The inverted stereo-configuration of C8a is important to SW's potent α-D-mannosidase inhibition, as the inhibitory activity of (–)-8a-*epi*-swainsonine decreases by 7%.[23,24]

In 2017, Schardl and colleagues identified the conserved biosynthetic gene clusters (BGCs) for SW in fungi (**Figure 1b**). The SW BGC features a nonribosomal peptide-polyketide synthase (NRPS-PKS) hybrid (SwnK), two non-heme iron and α-ketoglutarate (Fe/αKG)-dependent oxygenases (SwnH1 and SwnH2), two NAD(P)H-dependent oxidoreductases (SwnN and SwnR), and occasionally a transporter (SwnT) and a pyridoxal 5'-phosphate (PLP)-dependent aminotransferase (SwnA).[25] Based on predicted gene functions and Harris's feeding study, Schardl et al. proposed a plausible biosynthetic pathway for SW, where SwnK makes the indolizidine scaffold while other enzymes (e.g. oxygenase and reductase) are responsible for the tailoring steps (**Figure S1**). However, the exact function of each enzyme remains uncharacterized. Recently, Wang and coworkers conducted gene-deletion experiments and suggested a multibranched biosynthetic pathway for SW (**Figure S1**).[26] While this study offered insights, the multibranched proposal is contentious, as it contradicts several key findings by Harris. For instance, early feeding experiments indicated no epimerization at C1 in SW biosynthesis,[21] whereas the multibranched pathway involves multiple C1-epimer intermediates. Moreover, several critical questions remain unresolved, such as the mechanism underlying the epimerization process.

To address the long-standing questions about the biosynthetic mechanism of SW and reconcile discrepancies in the literature, we reconstituted the complete SW biosynthetic pathway both in vivo and in vitro. We established the biochemical basis for each enzyme involved in SW biosynthesis, uncovering that SW biosynthesis is far more complex than previously assumed. Our study demonstrates that the net redox-neutral epimerization is realized through an oxidation-reduction cascade, interrupted by a hydroxylation event that

dictates the stereochemical outcome of the reduction step. Insights gained from the characterization of these tailoring enzymes facilitated the biocatalytic synthesis of a novel polyhydroxylated indolizidine alkaloid, opening avenues for the future biosynthesis of diverse natural product-based glycosidase inhibitors.

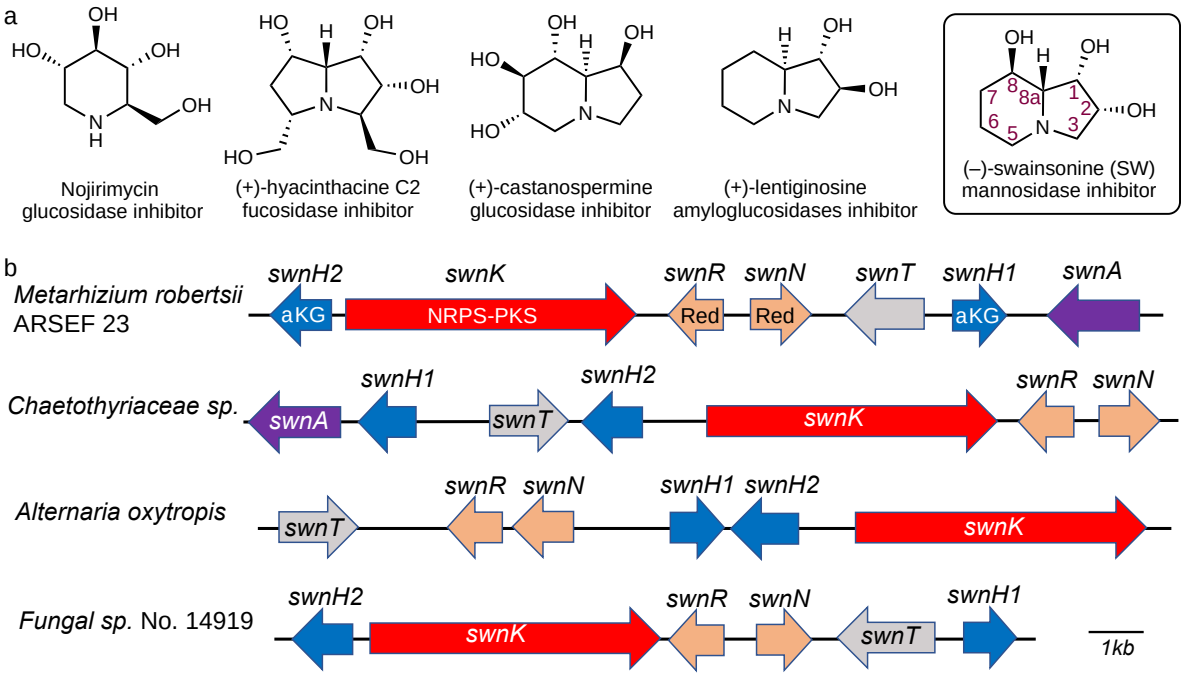

Figure 1. (–)-Swainsonine and other polyhydroxylated alkaloids. (A) Examples of polyhydroxylated alkaloids. (B) Swainsonine biosynthetic gene clusters from selected fungal species.

Results

Heterologous reconstitution of SW biosynthesis in vivo

We initiated our study by reconstructing the SW biosynthetic pathway in *Aspergillus nidulans* LO7890 (**Figure 2a**).[27] Expression of the NRPS-PKS hybrid SwnK alone did not yield any detectable products. However, supplementing the medium with L-PA or co-expressing the aminotransferase SwnA yielded 1-hydroxyindolizidine (**1**), indicating that *A. nidulans* LO7890 lacks endogenous L-PA and that SwnA is required for L-PA biosynthesis (**Figure S2**). Introducing the oxidoreductase SwnN and SwnR, subsequently raised the titer of compound **1** from 14 mg/L to 40 mg/L and 114 mg/L, respectively. To investigate whether this titer increase stemmed from enhanced L-PA availability, we dropped out *swnA* gene and supplemented exogenous L-PA to bypass its biosynthesis. A similar increase in titer by SwnR was still observed (**Figure S2**). In addition, expressing SwnA alone was sufficient to produce L-PA in *A. nidulans,* and co-expression with SwnR or SwnN did not further increase L-PA levels (**Figure S2**). These findings together indicate that neither SwnR nor SwnN participates in L-PA biosynthesis and that the increased titer of **1** by SwnR/SwnN is not due to enhanced supply of L-PA.

Adding the two Fe/αKG-dependent oxygenases, SwnH2 and SwnH1, to the expression system harboring *swnAKRN* resulted in the formation of intermediate 1,2-dihydroxyindolizidine (**2**) and, ultimately, the final product SW (**Figure 2a**). All compounds were isolated and characterized using NMR, high-resolution mass-spectrometry (MS) and optical rotation measurements (see **supplementary information**). Notably, we did not observe any epimers of **1** and **2** as previously reported.[26] We propose that the C1-epimers reported by Wang et al.[26] are conformational isomers rather than diastereomers (**Figure S4**). Our study demonstrated that although SwnR enhances the production of **1**, it is not essential for SW biosynthesis. Dropping out *swnR* gene resulted in a reduced yield of **1**, but the levels of **2** and

SW remained unchanged (trace vi, **Figure 2a**). On the contrary, removal of *swnH1* or *swnN* completely abolished SW production, leaving only intermediates **1** and **2** detectable (trace v and vi, **Figure 2a**). Similarly, removing *swnH2* stalled the pathway at **1** (trace x, **Figure 2a**). These results highlight that SwnH2, SwnH1, and SwnN are indispensable for SW biosynthesis.

To gain further insight into these enzyme functions, we fed isolated intermediates (**1** and **2**) to *A. nidulans* strains harboring different combinations of *swn* genes (**Figure 2b, 2c**). The strain expressing SwnH2 completely consumed **1** (trace iii, **Figure 2b**), but no product was detected unless SwnN was also present (trace v, **Figure 2b**). Similarly, feeding **2** to the strain expressing SwnH2 alone resulted in its consumption without forming detectable new products (trace ii, **Figure 2c**). However, with SwnN co-expressed, **2** seemed to be unaffected (trace v, **Figure 2c**). To our surprise, SwnH1 could also transform **2**, albeit less efficiently than SwnH2 (trace iii, **Figure 2c**). When SwnH1 and SwnN were co-expressed, **2** was partially converted into SW (trace v, **Figure 2c**), and complete conversion when SwnH2 was also present (trace vi, **Figure 2c**). These perplexing findings could not be explained by current biosynthetic proposals (**Figure S1**), underscoring that the swainsonine biosynthesis is more complex than previously anticipated.

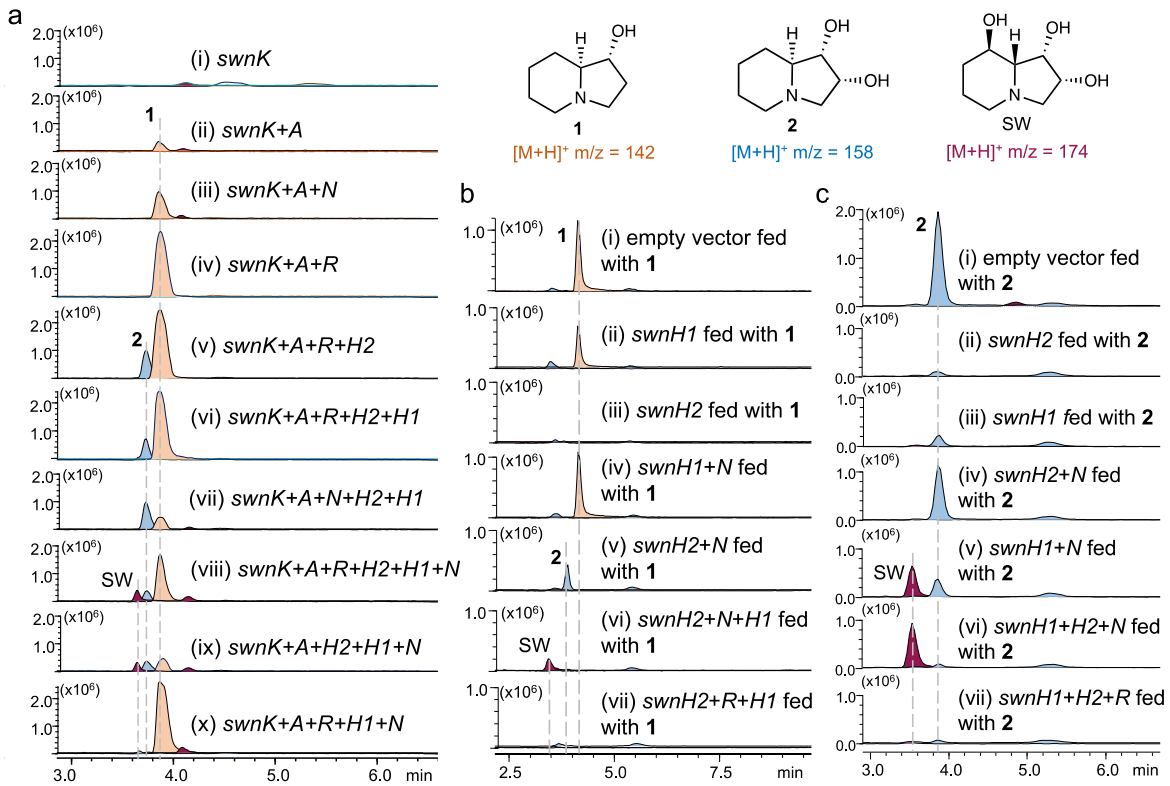

Figure 2. Reconstitution of swainsonine biosynthesis in *Aspergillus nidulans*. (a) LC-MS analysis of product profiles obtained from heterologous expression of different combinations of *swn* genes. (b) Feeding of intermediate **1** to *A. nidulans* transformed with different combination of *swn* genes. (c) Feeding of intermediate **2** to *A. nidulans* transformed with different combination of *swn* genes.

SwnA is a lysine 2-aminotransferase

To fully clarify the biosynthetic mechanism for SW and unambiguously determine each enzyme function, we next undertook in vitro characterization of each enzyme. We overexpressed SwnA, SwnR, SwnN, SwnH2, and SwnH1 in *E. coli*, and SwnK in *Saccharomyces cerevisiae* BJ5464-npgA strain.[28] Each protein was purified to homogeneity using metal-affinity chromatography followed by size-exclusion chromatography (**Figure S5**). We first examined the function of SwnA, which was proposed as a lysine 6-aminotransferase.[26] When SwnA was incubated with L-lysine and αKG, the expected lysine transamination reaction took place **(Figure 3a**). However, when we chemically reduced the reaction product (i.e. dehydropipecolic acid) with $NaBH_3CN$, we obtained a racemic mixture of pipecolic acids (**Figure 3b**). The loss of the L-configuration at the Cα position indicates that the enzymatic product of SwnA is actually 1-piperideine-2-carboxylate (P2C), rather than the previously proposed 1-piperideine-6-carboxylate (P6C). If P6C was the true product, chemical reduction would have preserved the stereochemical configuration, resulting in L-pipecolic acid. To further validate this finding, we repeated the reaction using different ^{15}N-labeled L-lysine substrates. After Fmoc-derivatization and mass analysis, the resulting ketoacid product showed a +1 Da mass shift with $^{15}N_{\varepsilon}$-L-lysine as the substrate, but not with $^{15}N_{\alpha}$-L-lysine (**Figure 3c**). Likewise, feeding $^{15}N_{\varepsilon}$-L-lysine to transformed *A. nidulans* strains led to partial isotope-incorporation into L-PA and **1**, whereas no mass change occurred with $^{15}N_{\alpha}$-L-lysine (**Figure S6**). Together, these results confirm that the α-amino group of L-lysine is lost during the SwnA-catalyzed transamination step. Therefore, SwnA is a lysine 2-aminotransferase rather than a lysine 6-aminotransferase as previously proposed.[26]

We also performed SwnA-coupled enzymatic assays with SwnN and SwnR to confirm that neither of them acts as a P2C reductase (**Figure S7**). While increasing the enzyme concentrations of SwnN and SwnR to 50 μM resulted in detectable pipecolic acid production,

the activities of both enzymes were insufficient to be considered physiologically relevant. In addition, SwnR exhibited poor enantioselectivity, whereas SwnN predominantly produced the undesired enantiomer, D-PA. Together, these findings suggest that some endogenous imine reductase(s) in the fungal host likely fulfills the role of dehydropipecolic acid reductase required for L-PA biosynthesis.

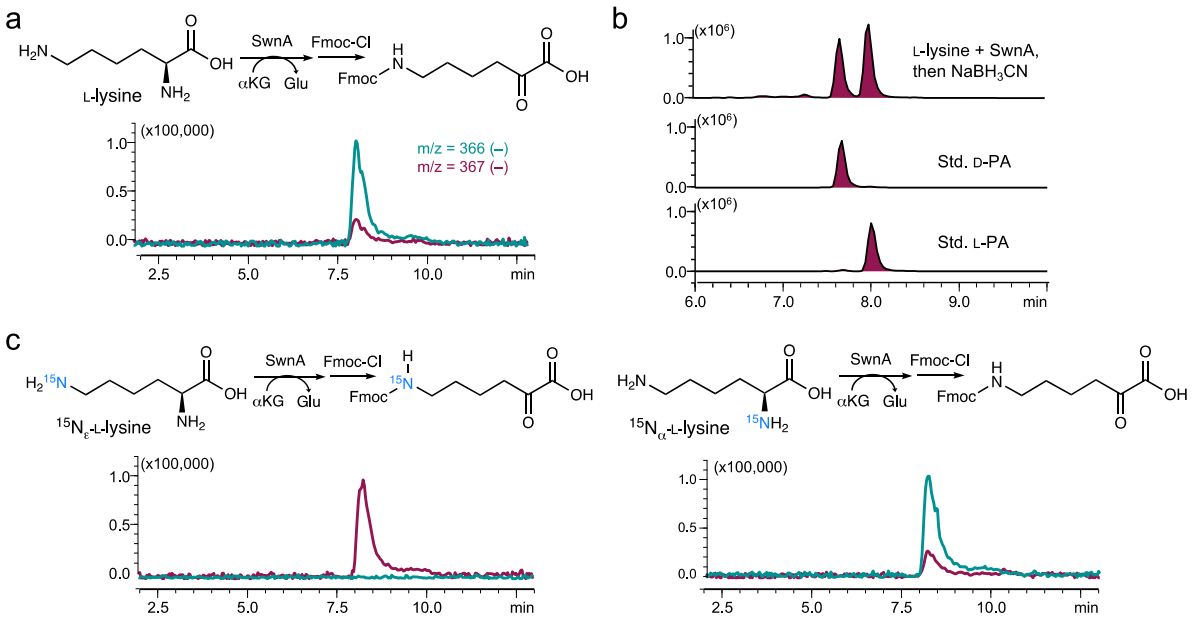

Figure 3. SwnA is a lysine 2-aminotransferase. (a) Fmoc-derivatization of SwnA-catalyzed transamination product from L-lysine. (b) Chiral analysis of the chemically reduced SwnA enzymatic product after derivatization with Marfey reagents. (c) Isotope-labeling experiment confirms that SwnA is a lysine 2-aminotransferase.

Reconstitution of indolizidine backbone biosynthesis of SW in vitro

Following the function elucidation of SwnA, we next focused on SwnK, the enzyme responsible for constructing the indolizidine scaffold of SW. When provided with the necessary substrates and cofactors (i.e. malonyl-CoA, NADPH, and pipecolic acid), SwnK readily synthesized **1** in vitro, demonstrating a clear preference for L-PA over D-PA as the amino acid substrate (**Figure S8**). The ability of SwnK to produce **1** from L-PA alone is consistent with the in vivo result that **1** was produced when only SwnK and SwnA were co-expressed (trace ii, **Figure 2a**). These results confirm that SwnK, rather than the previously proposed SwnN,[26] determines the stereochemistry of the C1-OH in **1**.

To investigate why SwnR significantly enhances the fermentation titer of **1**, we reperformed metabolomics analysis using GC-MS. Alongside **1,** we identified a new metabolite, 5,6,7,8-tetrahydroindolizine (**3**), in the cell cultures of *A. nidulans* co-expressing SwnK and SwnA (**Figure S9**). When either SwnR or SwnN was included, the amount of **3** became negligible. We propose that **3** is derived from **4**, an iminium precursor of **1** (**Figure S9**). Without immediate reduction of the cyclic iminium moiety in **4**, it undergoes dehydration and isomerization to give the shunt product **3**. Therefore, although SwnK is able to reduce **4** to yield **1**, efficient reduction of **4** in vivo likely requires a dedicated imine reductase. Given that introducing *swnR* resulted in the highest yield of **1**, SwnR is likely the primary imine reductase for **4**, enhancing production of **1** by minimizing formation of **3**. In the absence of SwnR, SwnN can partially fulfill this role, but with less efficiency.

Elucidating the epimerization process of SW biosynthesis

To unravel the sequential enzymatic transformations in the tailoring phase of SW biosynthesis, we first investigated SwnH2, which was demonstrated to act on both **1** and **2** in vivo (**Figure 2c** and **Figure 2d**). When supplied with the necessary cofactor and co-substrates

(e.g. αKG, ferrous sulfate, sodium ascorbate), SwnH2 efficiently oxidized **1** to **2** while concurrently generating a new compound **5** (trace i, **Figure 4a**). Structural analysis identified **5** as the iminium derivative of **1** (**Table S6**), and the ratio between **2** and **5** were determined to be approximately 4.9:1 (**Figure S10**). In agreement with in vivo observations, SwnH2 further oxidized **2** (trace iv and v, **Figure 4a**), yielding two new species, **6** and **7** (m/z(+) = 156 and 174, respectively). Isolation and structural analysis revealed that **6** is the iminium derivative of **2** (**Table S7**), while **7** was proposed as the equilibrated hemiaminal form of **6**, based on its reduction by $NaBD_3CN$ (**Figure S12**). The fact that SwnH2 can sequentially oxidize **1** and **2** demonstrate that SwnH2 is a bifunctional enzyme capable of catalyzing both C2-hydroxylation and a formal amine desaturation reaction.

During the isolation process, **6** spontaneously isomerized, resulting in a mixture of **6** and its epimer, 2-*epi*-**6** (**Figure S11**). The instability likely explains why **6** was undetectable during in vivo studies (e.g. trace v, **Figure 4a**). Treatment of an isolated sample of **6** (containing 33 mol% 2-*epi*-**6**) with SwnN and NADPH led to iminium reduction, producing a species with the molecular weight (m/z(+) = 158) and retention time resembling **2** (trace i, **Figure 4b**). Isolation and structural analysis revealed this species to be a ~1:1 mixture of two diastereomers: **2** and its epimer, 2-*epi*-**2** (**Figure S13**). As controls, neither SwnR nor boiled SwnN could reduce **6,** confirming that NADPH alone is insufficient to reduce the iminium compound **6** under these assay conditions (trace ii and iii, **Figure 4b**). We hypothesize that 2-*epi*-**2** arose from 2-*epi*-**6**, an artifact generated during the isolation of **6**. The fact that SwnN can reduce **6** back to **2** aligns with our feeding experiments, where **2** was consumed by SwnH2 but accumulated in the presence of both SwnH2 and SwnN. The absence of 8a-*epi*-**2** in the isolated enzymatic products indicates that SwnN specifically reduces **6** via the α-face.

Recognizing that reduction of **6** is not the correct timing for epimerization, we explored the alternative sequence where C8-hydroxylation precedes imine reduction. When the same

sample of isolated **6** was treated with SwnH1 and the necessary cofactor and co-substrates, rapid consumption of **6** was observed. A new species, **8**, appeared at early time points (trace iv, **Figure 4b**). Chemical reduction of **8** by $NaBH_4$ suggested that it is an iminium compound (**Figure S14**). Including SwnN and NADPH in the reaction enabled enzymatic reduction of **8** (trace v, **Figure 4b**), yielding the final product SW (**Figure S15**). Structural analysis of the isolated enzymatic reaction products also revealed 2-*epi*-**2**, presumably derived from the artifact 2-*epi*-**6** mixed in the substrate sample (**Figure S15**).

These findings strongly suggest the following: (1) SwnH1 catalyzes stereospecific C8-hydroxylation to produce an iminium triol intermediate **8**; (2) SwnN reduces **8** through its β-face, completing the enigmatic stereoinversion. Given that SwnN also reduces **6** to **2**, these findings together indicate that SwnN is a rare imine reductase displaying substrate-dependent stereospecificity, capable of setting opposite stereochemistry with different substrates. Notably, this behavior contrasts with the non-stereospecific hydride transfer catalyzed by many sugar epimerases, such as UDP-hexose-4-epimerase, which reduces transient keto intermediates in a non-stereospecific manner to yield either UDP-galactose or UDP-glucose.[29]

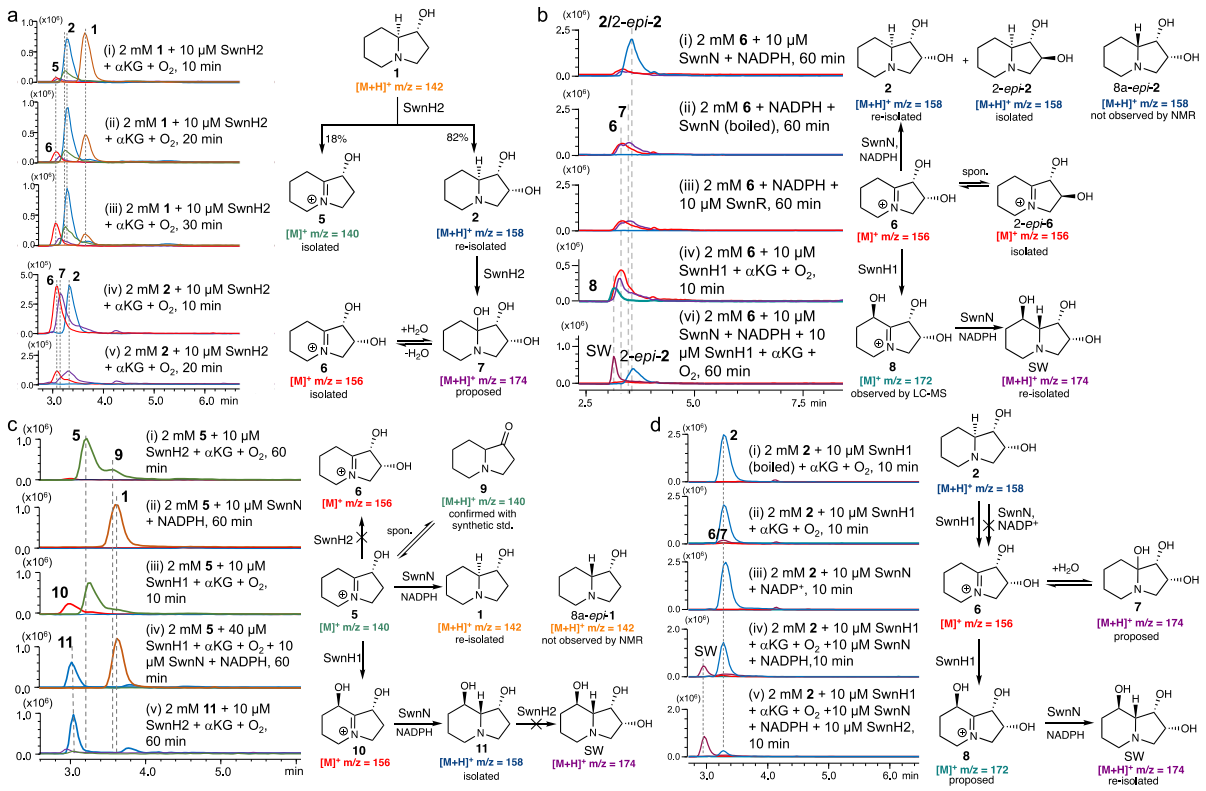

Figure 4. Elucidating the tailoring phase of swainsonine biosynthesis involving enzymes SwnH2, SwnH1, and SwnN. (a) SwnH2-catalyzed oxidation of **1** and **2**. (b) Establishing the intermediacy of **6**. (c) Iminium compound **5** is a shunt product, but can be recycled by SwnN to regenerate **1**. (d) SwnH1-catalyed oxidation of **2.**

Timing of epimerization is determined by C8-hydroxylation

Having established the intermediacy of **6** in SW biosynthesis, we next focused on **5**, another iminium compound derived from **1**, to assess its potential role as an intermediate in SW biosynthesis. Compound **5** was neither oxidized by SwnH2 (trace i, **Figure 4c**) nor reduced by SwnR (**Figure S16**). Instead, under these conditions, **5** spontaneously tautomerized to its ketone isomer, **9** (**Figure S16**). In contrast, SwnN successfully reduced **5** using NADPH (trace ii, **Figure 4c**), producing **1** as a single diastereomer product, with no detectable formation of 8a-*epi*-**1** in the isolated product.

Interestingly, SwnH1 hydroxylated **5** to produce a new iminium compound **10** (trace iii, **Figure 4c**). When **10** was further reduced by SwnN, a new diol compound **11** was isolated and identified as 2-deoxy-swainsonine (trace iv, **Figure 4c**). However, SwnN-catalyzed reduction of **5** outcompetes SwnH1-catalyzed hydroxylation of **5** (**Figure S17**). Therefore, elevated enzyme concentrations ($\geq$ 40 μM) of SwnH1 were required to enable successful isolation of **11**, suggesting **5** is not a native substrate of SwnH1. Compound **11** was not a kinetically competent intermediate for SW biosynthesis, as incubation with SwnH2 produced only trace amounts of a triol product (trace v, **Figure 4C**). Overall, these results demonstrate that **5** is not an on-pathway intermediate for SW biosynthesis, but it can be recycled by SwnN to regenerate intermediate **1**. Nevertheless, the stereochemistry of **11** fully matches that of SW, confirming that 1) SwnH1 stereo-specifically installs the C8-OH group on **5** at its β-face, as it does with its native-substrate **6**; 2) SwnN reduces the iminium compound **10** from its β-face.

Comparing SwnN-catalyzed iminium reductions revealed that, while SwnN establishes the stereochemistry at the ring fusion, the ultimate stereochemical outcome is dictated by SwnH1. When SwnH1 installs the C8-OH group at the β-face-, SwnN preferentially reduces the substrates from the same face, yielding C8a-epimerized products (e.g. **11** and SW). In contrast, without the SwnH1-installed C8-OH group (e.g. **5** or **6**), SwnN reduces the

iminium substrates from the α-face. To understand the structural basis for this unusual substrate-dependent stereoselectivity, we obtained an AlphaFold model of SwnN in complex with $NADP^+$,[30] and docked various products (e.g. **1**, **2**, **11**, and SW) into the active site pocket (**Figure S18**). The docking models suggest that SwnN recognizes the β-face oriented C8-OH group through a hydrogen bond, positioning the substrate for β-face reduction. In the absence of this anchoring group, substrates bind with a flipped-ring orientation, using the C1-OH group to form similar hydrogen bonds, leading to α-face reduction.

SwnH2 and SwnH1 are bifunctional enzymes

After ruling out the pathway branching from **5** to SW, we turned our attention to another unexpected finding from our in vivo studies. Specifically, SwnH1 was shown to utilize compound **2** in vivo (trace iii, **Figure 2c**), and in the presence of both SwnH1 and SwnN, **2** was partially converted to SW (trace v, **Figure 2c**). While SwnN was unable to oxidize **2** (trace iii**, Figure 4c**), SwnH1 successfully oxidized **2** to produce **6**/**7** (trace ii**, Figure 4c**). However, the yield of **6** in the reaciton was insufficient for structural confirmation. In a one-pot reaction containing both SwnN and SwnH1, a clear transformation of **2** into SW was observed (trace iv, **Figure 4c**). With SwnH2 was also included in this reaction, complete conversion of **2** was achieved (trace v, **Figure 4c**), consistent with results from our feeding study. No 2-*epi*-**2** was found in the product isolated from this biocatalytic cascade (**Figure S15**), further confirming that 2-*epi*-**2** and its precursor, 2-*epi*-**6**, are unrelated to the natural biosynthetic pathway, and these artifacts are not formed when intermediate **6** is generated in situ.

These results establish that SwnH1 is also a bifunctional enzyme. However, unlike SwnH2, which cleaves two C-H bonds exclusively at the α-face, SwnH1 breaks C-H bonds on opposite faces (e.g. β-oriented C_8-H bond and α-oriented C_{8a}-H bond). We propose that SwnH2 can catalyze hydrogen-atom abstraction and oxygen-rebound at both C2 and C8a

because the ferryl intermediate approaches substrate from the α-face. The bifurcation is likely determined by the relative distance between C_2-H/C_{8a}-H bond and the ferryl intermediate. In contrast, for SwnH1, similar hydrogen atom transfer (HAT) at C8a is not feasible, as the ferryl intermediate likely approaches the substrate from the β-face (**Figure S19**). This hypothesis is supported by enzymatic reactions performed using C8a-deuterium labeled **2**, which revealed a clear primary kinetic isotope effect with SwnH2 but not with SwnH1 (**Figure S20**). Therefore, while both enzymes catalyze the same formal amine desaturation reaction, they should proceed through distinct mechanistic pathways.

Directing SwnH2 function by a protecting/directing group

Acetylation is a common protective strategy in natural product biosynthetic pathways, resulting in cryptic acetylated biosynthetic intermediates that are unforeseeable without biosynthetic investigation.[31,32] Accordingly, we also hypothesized that a similar cryptic acetylation-deacetylation event may be involved in swainsonine biosynthesis. To test this, we synthesized *O*-acetylated-**1** (**Ac**-**1**) and evaluated its relevance to SW biosynthesis using purified enzymes. No reaction was observed with SwnH1 (trace i, **Figure 5**). However, SwnH2 successfully converted **Ac**-**1** into an acetylated diol product (**Ac**-**12**) and the shunt product **5** (trace ii and iii, **Figure 5**). Structural characterization of **Ac**-**12** revealed an α-face-oriented hydroxyl group at C7. These results eliminate the possibility of **Ac-1** serving as a biosynthetic intermediate in SW biosynthesis. Nonetheless, the stereochemistry of the C7-OH group in **Ac**-**12** supports our proposed mechanism, where substrates approach the non-heme iron center in SwnH2 via the α-face (**Figure S19**).

Given the removable nature of the *O*-acetyl group, we next subjected the deprotected diol, **12**, to further oxidative tailoring by SwnH2. SwnN and NAPDH were included in the reaction to quench any unstable iminium intermediates. From this biocatalytic cascade, we

successfully isolated a triol compound, **13** (trace v, **Figure 5**). Structural analysis identified **13** as a novel polyhydroxylated indolizidine alkaloid, isomeric to SW, with the same C2-OH group but lacking C8a epimerization. The absence of epimerization supports our gatekeeping mechanism, which posits that epimerization occurs only after SwnH1 installs the C8-OH group.

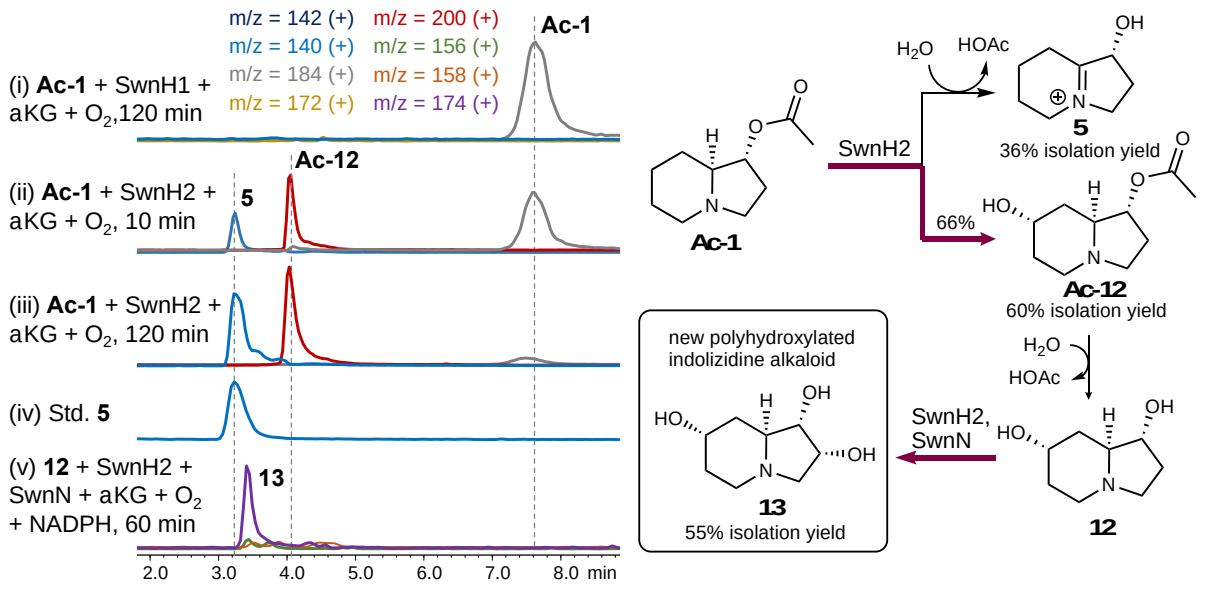

Figure 5. Biocatalytic synthesis of a novel polyhydroxylated indolizidine alkaloid enabled by a protective acetyl group-directed biosynthesis.

Discussion

Polyhydroxylated alkaloids are renowned for their potent glycosidase inhibitory activities and potential therapeutic applications, yet their biosynthetic pathways remains largely unexplored. Our study of the SW biosynthesis marks the first complete elucidation of the biosynthetic pathway of any polyhydroxylated alkaloid to date. Contrary to the multibranched pathway proposed by Wang et al.,[26] our findings support a linear biosynthetic mechanism in agreement with feeding studies conducted four decades ago.[21] Briefly, the NRPS-PKS hybrid SwnK constructs the indolizidine backbone from L-pipecolic acid, while the tailoring enzymes (SwnH2, SwnH1, and SwnK) catalyze late-stage modifications: C2-hydroxylation, amine desaturation, C8-hydroxylation, and imine reduction, culminating in the production of SW (**Figure 6**).

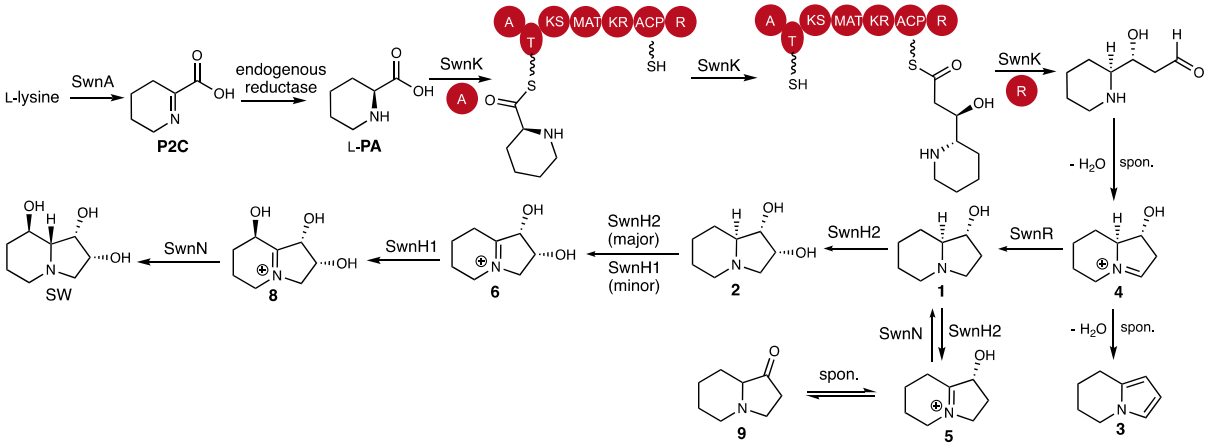

Figure 6. Revised swainsonine biosynthetic pathway based on the findings from this study.

The sequential oxidation-reduction process is a common chemical logic for stereoinversion in both chemical synthesis and biosynthesis.[33-35] The epimerization process in SW biosynthesis elucidated here is reminiscent of the conversion of (*S*)-reticuline to (*R*)-reticuline via 1,2-dehydroreticuline in morphine biosynthesis.[36] Unlike reticuline epimerase, a fusion protein consisting a cytochrome P450 domain and an aldo-keto reductase domain, SW biosynthesis recruits three separate enzymes to achieve stereoinversion. Notably, the stereochemical outcome of imine reduction is dictated by SwnH1-catalyzed hydroxylation, adding an additional layer of stereochemical control at the ring fusion. This complexity enables a single reductase, SwnN, to function in both epimerization and recycling of the byproduct **5**. Reductases exhibiting such substrate-dependent stereospecificity are exceedingly rare. While a few ketoreductases within PKS assembly lines show similar behaviors,[37,38] SwnN is the first standalone imine reductase capable of substrate-dependent stereospecific reduction.

The serendipitous enzymatic synthesis of (Ac)-**12** and its derivative **13** highlights the role of an artificially attached *O*-acetyl group, which functions not only as a protecting group to prevent hydroxylation at C2, but also as a directing group, altering the site-selectivity of SwnH2 while maintaining stereoselectivity. We propose that the bulky acetyl group induces a subtle shift in substrate binding, rendering the C_2-H bond inaccessible while positioning the C7 site closer to the ferryl intermediate.[39] Although the detailed mechanism of SwnH2 remains to be fully elucidated, our ability to successfully alter the site-selectivity of SwnH2 using a detachable protecting group is noteworthy. This approach suggests a general strategy for biocatalysis, where deploying detachable protecting groups to direct enzyme activity may serve as a practical alternative to engineering the enzymes themselves.[40]

Finally, our study of SW biosynthesis sheds light on the biosynthetic pathway of slaframine, a structurally related indolizidine alkaloid (**Figure S21**). Like SW, slaframine is also derived from L-pipecolic acid, and the fungus *R. leguminiocola* produces both SW and slaframine. Harris et al. proposed that slaframine and SW share a common early biosynthetic

pathway, with ketone indolizidine **9** serving as a shared precursor.[21] However, our findings show that **9** is not a biosynthetic intermediate for SW, and the C1-OH stereochemistry in SW is determined by SwnK. These results suggest that the existence of a separate NRPS-PKS hybrid dedicated to slaframine biosynthesis in *R. leguminiocola*, likely similar to SwnK but with a distinct ketoreductase domain that determine the opposite stereochemistry of the C1-OH. Here we propose a revised biosynthetic pathway for slaframine, informed by our discoveries in SW biosynthesis (**Figure S21**).

Conclusion

In conclusion, we have elucidated the complete biosynthesis of swainsonine, solving a biosynthetic puzzle that has persisted for decades. Our comprehensive characterization of SwnH2, SwnH1, and SwnN unveiled an unusual epimerization mechanism: it follows a classic oxidation-reduction sequence interrupted by a hydroxylation event that ultimately determines the stereochemical outcome of the reduction step. We demonstrated that reductase SwnN exhibits unusual substrate-dependent stereoselectivity, while SwnH1 and SwnH2 are bifunctional (Fe/αKG)-dependent oxygenases and provided mechanistic insights. Additionally, we directed the site-selectivity of SwnH2 by deploying a protective acetyl group on the substrate. This strategy enabled the biosynthesis of a new polyhydroxylated alkaloid. Our study highlights the potential of harnessing these biosynthetic enzymes for the discovery and development of new natural product-based glycosidase inhibitors.

Data availability

All data supporting the findings of this study are presented in the main text and the Supplementary Information file. NCBI (https://www.ncbi.nlm.nih.gov/) accessions codes are referenced in the Supplementary Information file. All data is available from the corresponding author upon request.

Acknowledgements

This work is supported by the University of California Cancer Research Coordinating Committee Grant C24CR7230 and NIH grant R35GM151205. The authors thank Dr. Christopher Schardl (University of Kentucky) for helpful discussions, and Prof. Berl R. Oakley (University of Kansas) for providing A. nidulans strain LO7890, and Prof. Yi Tang (University of California, Los Angeles) for providing the S. cerevisiae BJ5464-npgA strain.

Author contributions:

Y.H. and S.L. designed the overall research. S.L. and Z.B. performed all biochemical experiments. Y.H. and S.L. wrote the manuscript.

Competing interests

The authors have no competing interests to declare.

References:

1 Watson, A. A., Fleet, G. W., Asano, N., Molyneux, R. J. & Nash, R. J. Polyhydroxylated alkaloids -- natural occurrence and therapeutic applications. *Phytochemistry* **56**, 265-295 (2001). https://doi.org:10.1016/s0031-9422(00)00451-9

2 Elbein, A. D. & Molyneux, R. J. in *Comprehensive Natural Products Chemistry* (eds Sir Derek Barton, Koji Nakanishi, & Otto Meth-Cohn) 129-160 (Pergamon, 1999).

3 Kim, Y. *et al.* Glycosidase-targeting small molecules for biological and therapeutic applications. *Chem Soc Rev* **52**, 7036-7070 (2023). https://doi.org:10.1039/d3cs00032j

4 Colegate, S., Dorling, P. & Huxtable, C. A Spectroscopic Investigation of Swainsonine: An α-Mannosidase Inhibitor Isolated from <I>Swainsona canescens</I>. *Australian Journal of Chemistry* **32**, 2257-2264 (1979). https://doi.org:https://doi.org/10.1071/CH9792257

5 Schneider, M. J., Ungemach, F. S., Broquist, H. P. & Harris, T. M. (1S, 2R, 8R, 8aR)-1, 2, 8-trihydroxyoctahydroindolizine (swainsonine), an α-mannosidase inhibitor from Rhizoctonia leguminicola. *Tetrahedron* **39**, 29-32 (1983).

6 Molyneux, R. J. & James, L. F. Loco Intoxication: Indolizidine Alkaloids of Spotted Locoweed (Astragalus lentiginosus). *Science* **216**, 190-191 (1982). https://doi.org:10.1126/science.6801763

7 Dorling, P. R., Huxtable, C. R. & Colegate, S. M. Inhibition of lysosomal alpha-mannosidase by swainsonine, an indolizidine alkaloid isolated from Swainsona canescens. *Biochem J* **191**, 649-651 (1980). https://doi.org:10.1042/bj1910649

8 Tulsiani, D. R., Harris, T. M. & Touster, O. Swainsonine inhibits the biosynthesis of complex glycoproteins by inhibition of Golgi mannosidase II. *J Biol Chem* **257**, 7936-7939 (1982).

9 Elbein, A. D., Solf, R., Dorling, P. R. & Vosbeck, K. Swainsonine: an inhibitor of glycoprotein processing. *Proc Natl Acad Sci U S A* **78**, 7393-7397 (1981). https://doi.org:10.1073/pnas.78.12.7393

10 Shaheen, P. E. *et al.* Phase II study of the efficacy and safety of oral GD0039 in patients with locally advanced or metastatic renal cell carcinoma. *Investigational New Drugs* **23**, 577-581 (2005). https://doi.org:10.1007/s10637-005-0793-z

11 White, S. L., Schweitzer, K., Humphries, M. J. & Olden, K. Stimulation of DNA synthesis in murine lymphocytes by the drug swainsonine: immunomodulatory properties. *Biochem Biophys Res Commun* **150**, 615-625 (1988). https://doi.org:10.1016/0006-291x(88)90437-8

12 Winkler, D. A. & Holan, G. Design of potential anti-HIV agents. 1. Mannosidase inhibitors. *J Med Chem* **32**, 2084-2089 (1989). https://doi.org:10.1021/jm00129a011

13 Tian, Y.-S. *et al.* Asymmetric Synthesis of (−)-Swainsonine. *The Journal of Organic Chemistry* **74**, 3962-3965 (2009). https://doi.org:10.1021/jo802800d

14 Lindsay, K. B. & Pyne, S. G. Asymmetric Synthesis of (−)-Swainsonine, (+)-1,2-Di-epi-swainsonine, and (+)-1,2,8-Tri-epi-swainsonine. *The Journal of Organic Chemistry* **67**, 7774-7780 (2002). https://doi.org:10.1021/jo025977w

15 Louvel, J., Chemla, F., Demont, E., Ferreira, F. & Pérez-Luna, A. Synthesis of (−)-Swainsonine and (−)-8-epi-Swainsonine by the Addition of Allenylmetals to Chiral α,β-Alkoxy Sulfinylimines. *Organic Letters* **13**, 6452-6455 (2011). https://doi.org:10.1021/ol202747p

16 Guo, H. & O'Doherty, G. A. De Novo Asymmetric Synthesis of d- and l-Swainsonine. *Organic Letters* **8**, 1609-1612 (2006). https://doi.org:10.1021/ol0602811

17 Zhou, W.-S., Xie, W.-G., Lu, Z.-H. & Pan, X.-F. Asymmetric formal total synthesis of (–)-swainsonine. *Journal of the Chemical Society, Perkin Transactions 1*, 2599-2604 (1995). https://doi.org:10.1039/P19950002599

18 Punniyamurthy, T., Irie, R. & Katsuki, T. Short step enantioselective synthesis of (-)-swainsonine. *Chirality* **12**, 464-468 (2000). https://doi.org:10.1002/(sici)1520-636x(2000)12:5/6<464::Aid-chir28>3.0.Co;2-z

19 Ceccon, J., Greene, A. E. & Poisson, J. F. Asymmetric [2 + 2] cycloaddition: total synthesis of (-)-swainsonine and (+)-6-epicastanospermine. *Org Lett* **8**, 4739-4742 (2006). https://doi.org:10.1021/ol0617751

20 Schneider, M. J., Ungemach, F. S., Broquist, H. P. & Harris, T. M. Biosynthesis of swainsonine in Rhizoctonia leguminicola. Epimerization at the ring fusion. *Journal of the American Chemical Society* **104**, 6863-6864 (1982). https://doi.org:10.1021/ja00388a102

21 Harris, C. M., Schneider, M. J., Ungemach, F. S., Hill, J. E. & Harris, T. M. Biosynthesis of the toxic indolizidine alkaloids slaframine and swainsonine in Rhizoctonia leguminicola: metabolism of 1-hydroxyindolizidines. *Journal of the American Chemical Society* **110**, 940-949 (1988). https://doi.org:10.1021/ja00211a039

22 Harris, C. M., Campbell, B. C., Molyneux, R. J. & Harris, T. M. Biosynthesis of swainsonine in the diablo locoweed (Astragalus oxyphyrus). *Tetrahedron Letters* **29**, 4815-4818 (1988). https://doi.org:https://doi.org/10.1016/S0040-4039(00)80616-4

23 Tadano, K.-i. *et al.* Synthesis of (−)-8a-epi-Swainsonine, (1S,2R,8R,8aS)-Octahydro-1,2,8-indolizinetriol. *Bulletin of the Chemical Society of Japan* **60**, 3667-3671 (2006). https://doi.org:10.1246/bcsj.60.3667

24 Tadano, K. *et al.* Syntheses of (-)-2,8a- and (-)-8,8a-di-epi-swainsonine and evaluation of their inhibitory activity against several glycosidases. *The Journal of Organic Chemistry* **53**, 5209-5215 (1988). https://doi.org:10.1021/jo00257a003

25 Cook, D. *et al.* Swainsonine Biosynthesis Genes in Diverse Symbiotic and Pathogenic Fungi. *G3 (Bethesda)* **7**, 1791-1797 (2017). https://doi.org:10.1534/g3.117.041384

26 Luo, F. *et al.* Unveiling of Swainsonine Biosynthesis via a Multibranched Pathway in Fungi. *ACS Chem Biol* **15**, 2476-2484 (2020). https://doi.org:10.1021/acschembio.0c00466

27 Chiang, Y. M. *et al.* Development of Genetic Dereplication Strains in Aspergillus nidulans Results in the Discovery of Aspercryptin. *Angew Chem Int Ed Engl* **55**, 1662-1665 (2016). https://doi.org:10.1002/anie.201507097

28 Bond, C. M. & Tang, Y. Engineering Saccharomyces cerevisiae for production of simvastatin. *Metab Eng* **51**, 1-8 (2019). https://doi.org:10.1016/j.ymben.2018.09.005

29 Frey, P. A. & Hegeman, A. D. Chemical and stereochemical actions of UDP-galactose 4-epimerase. *Acc Chem Res* **46**, 1417-1426 (2013). https://doi.org:10.1021/ar300246k

30 Abramson, J. *et al.* Accurate structure prediction of biomolecular interactions with AlphaFold 3. *Nature* **630**, 493-500 (2024). https://doi.org:10.1038/s41586-024-07487-w

31 Pan, J., Bhardwaj, M., Nagabhyru, P., Grossman, R. B. & Schardl, C. L. Enzymes from fungal and plant origin required for chemical diversification of insecticidal loline alkaloids in grass-Epichloë symbiota. *PLoS One* **9**, e115590 (2014). https://doi.org:10.1371/journal.pone.0115590

32 Liu, J., Ng, T., Rui, Z., Ad, O. & Zhang, W. Unusual Acetylation-Dependent Reaction Cascade in the Biosynthesis of the Pyrroloindole Drug Physostigmine. *Angewandte Chemie International Edition* **53**, 136-139 (2014). https://doi.org:https://doi.org/10.1002/anie.201308069

33 Suh, C. E., Carder, H. M. & Wendlandt, A. E. Selective Transformations of Carbohydrates Inspired by Radical-Based Enzymatic Mechanisms. *ACS Chemical Biology* **16**, 1814-1828 (2021). https://doi.org:10.1021/acschembio.1c00190

34 He, X., Agnihotri, G. & Liu, H.-w. Novel Enzymatic Mechanisms in Carbohydrate Metabolism. *Chemical Reviews* **100**, 4615-4662 (2000). https://doi.org:10.1021/cr9902998

35 Tanner, M. E. Transient oxidation as a mechanistic strategy in enzymatic catalysis. *Current Opinion in Chemical Biology* **12**, 532-538 (2008). https://doi.org:https://doi.org/10.1016/j.cbpa.2008.06.016

36 Farrow, S. C., Hagel, J. M., Beaudoin, G. A., Burns, D. C. & Facchini, P. J. Stereochemical inversion of (S)-reticuline by a cytochrome P450 fusion in opium poppy. *Nat Chem Biol* **11**, 728-732 (2015). https://doi.org:10.1038/nchembio.1879

37 Zhou, H. *et al.* A fungal ketoreductase domain that displays substrate-dependent stereospecificity. *Nature Chemical Biology* **8**, 331-333 (2012). https://doi.org:10.1038/nchembio.912

38 Schröder, M., Roß, T., Hemmerling, F. & Hahn, F. Studying a Bottleneck of Multimodular Polyketide Synthase Processing: the Polyketide Structure-Dependent

Performance of Ketoreductase Domains. *ACS Chemical Biology* **17**, 1030-1037 (2022). https://doi.org:10.1021/acschembio.2c00047

39 Krebs, C., Galonić Fujimori, D., Walsh, C. T. & Bollinger, J. M., Jr. Non-Heme Fe(IV)–Oxo Intermediates. *Accounts of Chemical Research* **40**, 484-492 (2007). https://doi.org:10.1021/ar700066p